International Journal of Heat and Mass Transfer 52 (2009) 5634–5642

Contents lists available at ScienceDirect

International Journal of Heat and Mass Transfer

journal homepage: www.elsevier.com/locate/ijhmt

Heat transportation by oscillatory flow in a new type of heat transportation pipe

Makoto Hishida *, Ryou Mitsuno, Xiaojin Zhang, Gaku Tanaka

Department of Mechanical Engineering, Graduate School of Engineering, Chiba University, Yayoi-cho, Inage-ku, Chiba-shi 263-8522, Japan

ARTICLE INFO

Article history:
Received 3 December 2008
Received in revised form 13 May 2009
Accepted 18 May 2009
Available online 17 August 2009

Keywords:
Longitudinal heat transportation
Oscillatory flow
Heat transportation pipe
Double tube

ABSTRACT

The present paper deals with experimental and numerical study on the longitudinal heat transportation by an oscillatory water flow in a double tube type heat transportation pipe. Experiments were performed to measure the heat transportation rate in the ranges of $2.3 \leqslant Wo \leqslant 7.2$ and $400 \leqslant Re_{max} \leqslant 6600$. The heat transportation rate was approximately 10–490 times the heat transportation rate of a straight round pipe, and it was around 1–40 times the heat conduction rate through a copper rod. Analytical heat transportation rates agreed well with the experimental ones.

1. Introduction

Small size heat transportation devices are currently required for the effective cooling of electronic devices and equipment due to the rapid growth of heat dissipation from integrated electric circuits. Heat transportation devices utilizing reciprocal flow are one of the important candidate technologies for this function.

Since the heat transportation pipe utilizing reciprocal flow was invented by Kurzweg and Zhao [1], many researchers have attempted to improve its performance. In this report, we call the oscillatory flow whose time-average flow rate in one cycle of oscillation is zero as the reciprocal flow. Kaviany [2] pointed out that the heat transportation of the reciprocal flow is enhanced by the utilization of unsteady heat transfer between the pipe wall and the reciprocal flow. Nishio et al. [3,4] investigated the conditions for achieving the optimum performance of the reciprocal flow heat transportation pipe: that is, they investigated extensively the effects of the thermal properties of the working fluid, the pipe diameter, the amplitude and frequency of the reciprocal flow, and the flow pattern (laminar or turbulent) on the heat transportation performance. They reported that water is the best working fluid because of its high effective thermal conductivity within a relatively wide range of reciprocal frequencies. They also pointed out that there is an optimum size for the heat transportation pipe. In addition, Nishio et al. [5] proposed a new kind of heat transportation pipe, an inverse oscillation-phase heat transport tube, which can achieve higher heat transportation performance than can a normal reciprocal-flow heat transportation pipe. Ohno et al. [6] proposed an annular-channel type heat transportation pipe which improved the heat transportation performance in a high frequency range. Inaba et al. [7] compared the heat transportation performance between the bundles of straight ducts with triangular, square and hexagonal cross-sections.

However, most of these previous studies have concentrated on the improvement of heat transportation through smooth straight pipes. Few studies have been performed on the heat transportation of the oscillatory flow in non-straight pipes, whose longitudinal shape is not straight.

We have been attempting to improve the heat transportation by changing the configuration of the oscillatory flow path or the longitudinal shape of the heat transportation pipe. If the non-straight pipes can produce new types of oscillatory flow which are suitable for the longitudinal heat transportation, it may be possible to improve the longitudinal heat transportation by employing the non-straight pipes.

For example, Ishii et al. [8] proposed a double tube type heat transportation pipe. They found by numerical simulation that a new oscillatory flow, whose time-average flow rate was not zero, was generated in a double tube by just imposing the reciprocal flow, whose time-average flow rate was zero, on one end of the double tube. They called the time-average flow component the unidirectional flow component. That is, the new oscillatory flow which they found in the double tube was composed of the reciprocal flow component and the unidirectional flow component (non-zero time-average flow component). They found that the unidirectional flow component greatly enhanced the longitudinal heat transportation of their new heat transportation pipe. Ishii et al. [9] also proposed a new heat transportation channel composed of a divergent and a convergent channel. They found that the new oscillatory flow, whose time-average flow rate was not zero, was also induced in the divergent and convergent channels by

* Corresponding author. Tel./fax: +81 43 432 6218.
E-mail address: iz5m-hsd@asahi-net.or.jp (M. Hishida).

0017-9310/$ - see front matter © 2009 Published by Elsevier Ltd.
doi:10.1016/j.ijheatmasstransfer.2009.05.018

Nomenclature

Am	tidal amplitude
d	inner diameter of the left circular orifice
f	frequency
q	total heat flux ($=\tilde{q}+\bar{q}$)
$\tilde{q}$	heat flux by the reciprocal flow component
$\bar{q}$	heat flux by the unidirectional flow component
Q	heat transportation rate
Q^*	dimensionless heat transportation rate ($=Q/Q_{ref}$)
$\mathrm{Re}_{\max}$	maximum Reynolds number ($=u_{\max}\cdot d/\nu$)
t	time
T	time period
u	flow velocity in x-direction
$\bar{V}$	flow rate of the unidirectional flow component
$u_{\max}$	maximum velocity of the reciprocal flow imposed at the left circular orifice
Wo	Womersley number ($=(d/2)\sqrt{2\pi f/\nu}$)
θ	temperature
θ^*	dimensionless temperature ($=(\theta-\theta_c)/(\theta_h-\theta_c)$)
$\Delta\theta$	temperature difference between the hot and cold water bathes ($=\theta_h-\theta_c$)

Subscripts

i	reciprocal flow imposed at the left circular orifice
inner	inner channel
outer	outer channel

imposing the reciprocal flow on one end of the new channel. They reported that the heat transportation rate of their new channel was higher than that of the straight channel because of the induced unidirectional flow component. On the other hand, Motoki et al. [10] investigated numerically the fluid movement and the heat transportation of the reciprocal flow in grooved ducts. They found that another new type of oscillatory flow was generated in the grooved duct. In the new oscillatory flow they observed violent longitudinal dispersion movements of the fluid. It should be mentioned that the normal reciprocal flow in the smooth straight ducts include no dispersion movements of fluid. They reported that the dispersion movements of the fluid caused the longitudinal enthalpy transportation and resulted in great augmentation of the longitudinal heat transportation of the reciprocal flow in the gloved ducts.

The above mentioned studies by Ishii et al. [8,9] and Motoki et al. [10] suggest that the longitudinal heat transportation of the reciprocal flow whose time-average flow rate is zero can be greatly enhanced by adding the unidirectional flow component on the reciprocal flow or by generating the longitudinal dispersion movements of fluid in the reciprocal flow.

The present study is an experimental investigation into the longitudinal heat transportation of a double tube type heat transportation pipe which was proposed by Ishii et al. [9] and investigating the flow and temperature fields by numerical analysis to discuss the heat transportation augmentation mechanism.

2. Experiments

2.1. Experimental set-up

Fig. 1(a) shows the experimental set-up, which mainly consisted of a test pipe, hot water bath, cold water bath, heat loss compensation water bath, constant temperature bathes and an apparatus generating the reciprocal flow. Heat generated by an electric heater in the hot water bath was transported to the cold water bath through the test tube. In order to minimize the heat loss from the hot water bath to the surroundings, the hot water bath was placed into the heat loss compensation water bath, whose temperature was kept at the same value as the hot water bath. Water in the heat loss compensation water bath was circulated through the constant temperature bath to keep its temperature constant. Thermal insulation material was wrapped around the test pipe. Copper tube coils were immersed in the cold water bath. Inside the coils, cold water with a constant temperature was circulated from the constant temperature bath. Revolution movement of the motor was converted to the reciprocal movement of the bellows by the Scoche and Yoke mechanism to generate the sinusoidal reciprocal flow with the tidal amplitude Am and frequency f (time period T). The sinusoidal reciprocal flow whose u-velocity in the longitudinal direction was expressed by Eq. (1), and it was imposed on the left end of the test tube.

$$u_i = u_{\max}\cdot\sin(2\pi ft) = 2\pi\cdot Am\cdot f\cdot\sin(2\pi ft) = 2\pi\cdot Am\cdot f\cdot\sin(2\pi t/T) \quad (1)$$

Fig. 1(b) shows the details of the hot water bath. Water temperature in the hot water bath was controlled by a PID temperature controller. The water in the hot water bath was circulated by a small pump in order to get a uniform water temperature in the hot water bath. The heat transportation rate Q of the present double tube type heat transportation pipe was evaluated by measuring the electrical heat input Q_{in} to the heater and adding the electrical power of the pump Q_{pump} = 2 W and subtracting the heat loss Q_{loss} from the experimental set-up to the surroundings. Q_{loss} was measured in the preliminary experiments. Thus Q was calculated by $Q = Q_{in} + Q_{pump} - Q_{loss}$. The heat loss Q_{loss} was less than 2.5% of the heat transportation rate Q.

Fig. 1(c) shows a rough drawing of the test pipe which consisted of an inner and an outer tube, a circular orifice at the left end and an annular orifice at the right end. The test pipe was made of acrylic resin material. The working fluid was water. The length L of the test tube was 241 mm. The inner and the outer diameter of the inner tube were 6 and 8 mm, respectively, and those of the outer tube were 14 and 18 mm. Four slits 15 mm long and 1 mm wide were opened at both ends of the inner tube. These slits connected the inner circular channel and the outer annular channel. The left circular orifice had a circular opening with a diameter of 6 mm and the right annular orifice had an annular opening with an outer diameter of 14 mm and an inner diameter of 8 mm. The right end of the test channel was connected to the hot water bath and the left end was connected to the cold water bath.

The Womersley number ($Wo = (d/2)\sqrt{2\cdot\pi\cdot f/\nu}$) and the maximum Reynolds number ($\mathrm{Re}_{\max} = u_{\max}\cdot d/\nu$) of the reciprocal flow imposed at the left end of the test channel were varied in the range of $2.3 \leqslant \mathrm{Wo} \leqslant 7.2$ and $400 \leqslant \mathrm{Re}_{\max} \leqslant 6600$ by varying the frequency f (or time period $T = 1/f$) in the range of $0.1 \leqslant f \leqslant 1.0$ Hz ($1 \leqslant T \leqslant 10$ s) and the amplitude of reciprocal flow Am in the range of $38 \leqslant Am \leqslant 190$ mm. The temperature of the hot water bath θ_h and the cold water bath θ_c were varied from 30 to 40 °C and 8 to 21 °C, respectively, and the temperature difference $\Delta\theta = \theta_h - \theta_c$ between the hot and cold bathes ranged from 9 to 29 °C. Here, d and ν are the inner diameter of the left circular orifice and the dynamic viscosity of water.

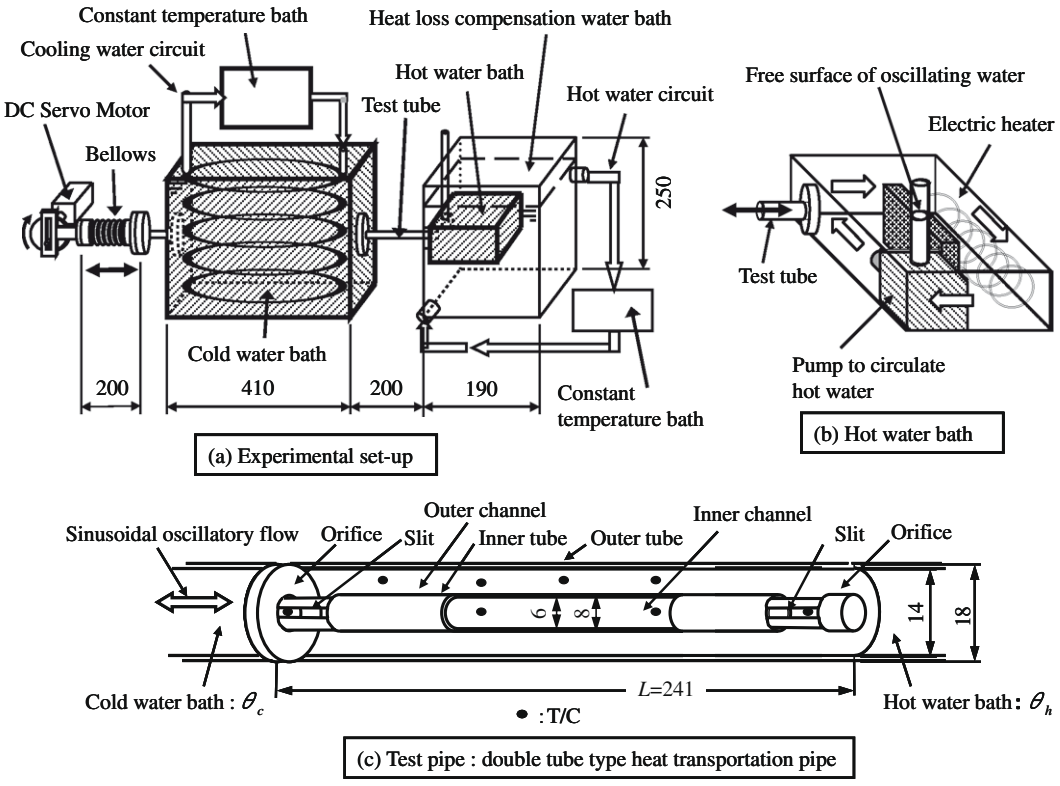

Fig. 1. Experimental set-up.

2.2. Experimental results

In Fig. 2, the heat transportation rates $Q/\Delta\theta = Q/(\theta_h - \theta_c)$ were plotted against the frequency f for the tidal amplitude of Am = 114 mm (circular symbols) and Am = 190 mm (triangular symbols). Our preliminary experiments revealed that Q was directly proportional to $\Delta\theta = \theta_h - \theta_c$. Fig. 2 shows that measured heat transportation rates increased in proportion to 1.3th power of the frequency and they were correlated by

$$Q/(\theta_h - \theta_c) = C \times f^{1.3}. \quad (2)$$

The dolled and dashed lines in Fig. 2 indicate the heat transportation rate $Q_{kav}/(\theta_h - \theta_c)$ of the straight round pipe with the same inner diameter (D = 14 mm) as that of the outer tube of the present double tube. Q_{kav} was calculated from the theoretical equation derived by Kaviany [2].

In Fig. 3, the heat transportation rates $Q/(\theta_h - \theta_c)$ were plotted against the tidal amplitude Am for f = 0.5 Hz (circular symbols) and f = 1.0 Hz (triangular symbols). The heat transportation rates increased in proportion to 1.3th power of the tidal amplitude, and they were correlated by

$$Q/(\theta_h - \theta_c) = C \times Am^{1.3}. \quad (3)$$

The dotted and dashed lines are the heat transportation rate of the straight round tube Q_{kav}.

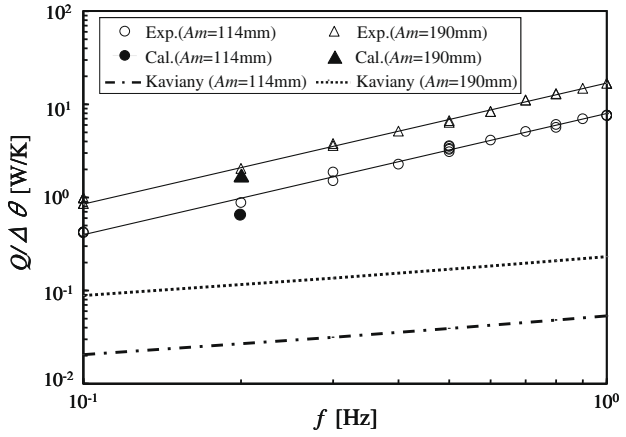

Fig. 2. Heat transportation rate against frequency of the reciprocal flow (Am = 114 mm, 190 mm).

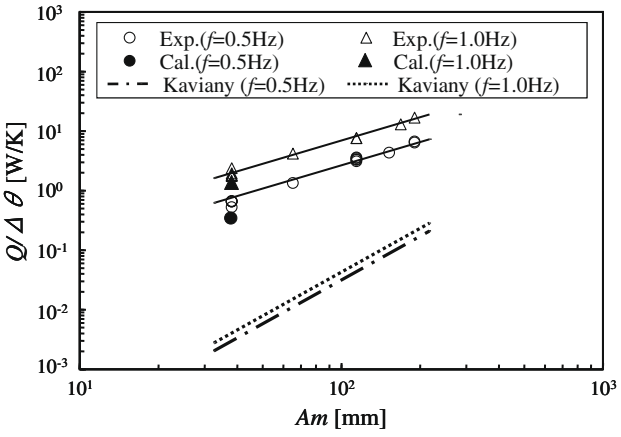

Fig. 3. Heat transportation rate against tidal amplitude of the reciprocal flow (f = 0.5 Hz, 1.0 Hz).

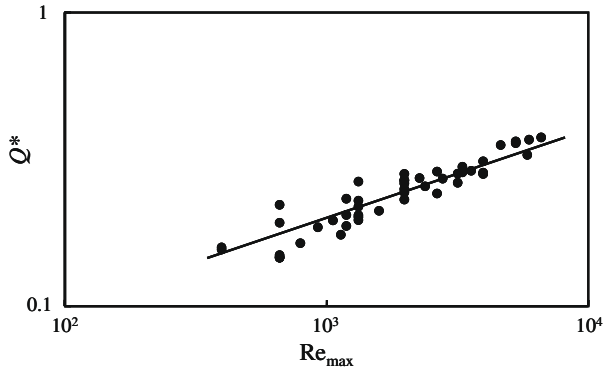

Fig. 4. Dimensionless heat transportation rate against maximum Reynolds number.

Figs. 2 and 3 show that the heat transportation rate Q of the present heat transportation pipe was about 10–490 times that of the straight round pipe Q_{kav}, and Q was around 1–40 times the heat conduction rate through the copper rod with the same outer diameter and length as those of the present double tube.

The black solid circular and triangular symbols in Figs. 2 and 3 are the calculated heat transportation rate, as will be described later. The calculated heat transportation rates agreed well with the experimental ones.

Fig. 4 plots the dimensionless heat transportation rate Q^* against Re_{max} Q^* was defined by the following equation:

$$Q^* = Q/Q_{ref} \tag{4}$$

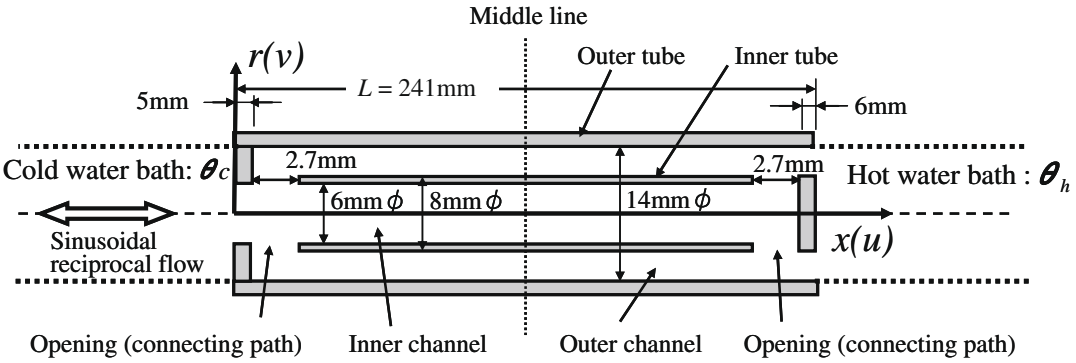

Fig. 5. Analytical model of present heat transportation pipe.

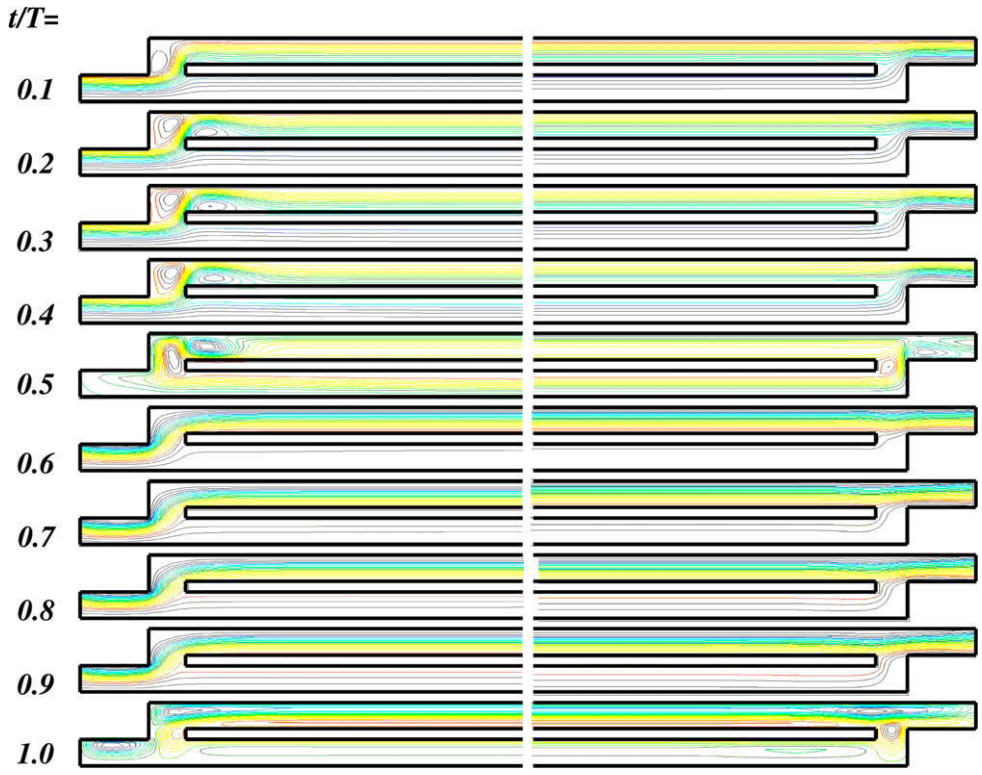

Fig. 6. Variation of contour lines of stream function in one cycle of oscillation in outer and inner channels (Am = 38.1 mm, f = 0.5 Hz).

$$Q_{ref} = -\rho C_p(\pi/4)d^2(\theta_h-\theta_c)\int_{0.5}^{1} u_i d(t/T)$$
$$= -\rho C_p(\pi/4)d^2(\theta_h-\theta_c)u_{\max}\int_{0.5}^{1}\sin(2\pi t/T)d(t/T)$$
$$= \rho C_p(\pi/4)d^2(\theta_h-\theta_c)u_{\max}(1/\pi) \quad (5)$$

Here, Q_{ref} means the longitudinal heat (enthalpy) transportation rate which can be transported from the hot to the cold water bath during the time of $0.5 \leqslant t/T \leqslant 1.0$ by the unidirectional convection flow given by Eq. (1).

Fig. 4 shows that Q^* of the present heat transportation pipe reached about 1/3 of $Q_{ref}Q^*$ of the present heat transportation pipe was roughly correlated by

$$Q^* = 0.0252\,\mathrm{Re}_{\max}^{0.3}. \quad (6)$$

3. Analysis

In order to investigate the heat transportation mechanism through the present heat transportation pipe, numerical analysis was performed.

3.1. Analytical model

Fig. 5 roughly sketches the analytical model for the present double tube type heat transportation pipe. The shape and the dimensions of the pipe were the same as those of the test pipe which was used in the present experiment. The only difference between the experimental and analytical test pipes was the connecting paths between the inner and outer channels, which were opened at both ends of the inner tube. The experimental test pipe had four slits opened in the inner tube at both ends as shown in Fig. 1(c), while the analytical model had circular gaps with the a gap distance of 2.7 mm at both ends as shown in Fig. 5. Both opening paths of the experimental and analytical pipes had the same opening area of approximately 60 mm^2.

Two-dimensional axially symmetric velocity and temperature fields were analyzed by solving the following conservation equations for mass, momentum and energy.

$$\frac{\partial u}{\partial x}+\frac{\partial v}{\partial r}+\frac{u}{r}=0 \quad (7)$$

$$\frac{\partial u}{\partial t}+u\frac{\partial u}{\partial x}+v\frac{\partial u}{\partial r}=-\frac{1}{\rho}\frac{\partial P}{\partial x}+\nu\left[\frac{\partial^2 u}{\partial x^2}+\frac{1}{r}\frac{\partial}{\partial r}\left(r\frac{\partial u}{\partial r}\right)\right] \quad (8)$$

$$\frac{\partial v}{\partial t}+u\frac{\partial v}{\partial x}+v\frac{\partial v}{\partial r}=-\frac{1}{\rho}\frac{\partial P}{\partial r}+\nu\left[\frac{\partial^2 u}{\partial x^2}+\frac{\partial}{\partial r}\left(\frac{1}{r}\frac{\partial(rv)}{\partial r}\right)\right] \quad (9)$$

$$\frac{\partial \theta}{\partial t}+u\frac{\partial \theta}{\partial r}+w\frac{\partial \theta}{\partial x}=\alpha\left[\frac{\partial^2\theta}{\partial x^2}+\frac{1}{r}\frac{\partial}{\partial r}\left(r\frac{\partial\theta}{\partial r}\right)\right] \quad (10)$$

The boundary conditions were given by

$$\text{at } x=0,\ u=u_{\max}\cdot\sin(2\pi t/T)=u_{\max}\cdot\sin(2\pi ft)=2\pi f\cdot Am\cdot\sin(2\pi ft),\ v=0,$$
$$\theta=\theta_c=285\ (\text{for } u\geqslant 0)\ \text{ and }\ \frac{\partial\theta}{\partial x}=0\ (\text{for } u<0) \quad (11)$$

Eq. (11) indicates that we delivered a sinusoidal reciprocal flow with frequency of f (or time period of T) and tidal amplitude of Am from the left end. Water with a uniform temperature of $\theta_c = 285$ K flowed into the pipe when $u \geqslant 0$ and water with $\partial\theta/\partial x = 0$ flowed out of the pipe when $u < 0$.

$$\text{at } x=L,\quad \frac{\partial u}{\partial x}=0,\ \frac{\partial v}{\partial x}=0,\ P=\text{constant},\ \frac{\partial\theta}{\partial x}=0\ (\text{for } u\geqslant 0)$$
$$\text{and }\ \theta=\theta_h=313\ (\text{for } u\leqslant 0) \quad (12)$$

Eq. (12) indicates that at the right end of the pipe, the pressure was constant and the velocity gradients were zero. The temperature boundary conditions at the right end were similar to those at the left end.

$$\text{at } r=0,\ \frac{\partial u}{\partial r}=0,\quad v=0,\ \frac{\partial\theta}{\partial r}=0 \quad (13)$$

at wall surfaces except those on the inner tube, $u=0$,

$$v=0,\ \frac{\partial\theta}{\partial r}=0\ \text{ and }\ \frac{\partial\theta}{\partial x}=0 \quad (14)$$

In order to consider the heat conduction from the outer to the inner channel through the inner acrylic tube, the heat conduction equation was solved by coupling with Eq. (10). Continuities of the temperature and heat flux were imposed on the inner and outer surface of the inner tube as the temperature boundary condition there. In order to investigate the effect of the heat conduction through the inner tube, we also performed an additional analysis for the analytical model with the complete adiabatic inner tube. In the additional analysis, Eq. (14) was imposed on all the wall surfaces as the velocity and temperature boundary conditions.

The analyses were performed for five sets of f and Am. They were (f = 1 Hz, Am = 38.1 mm), (f = 0.5 Hz, Am = 38.1 mm), (f = 0.2 Hz, Am = 38.1 mm), (f = 0.2 Hz, Am = 114 mm), (f = 0.2 Hz, Am = 190 mm). The computer code FLUENT [11] was used for the

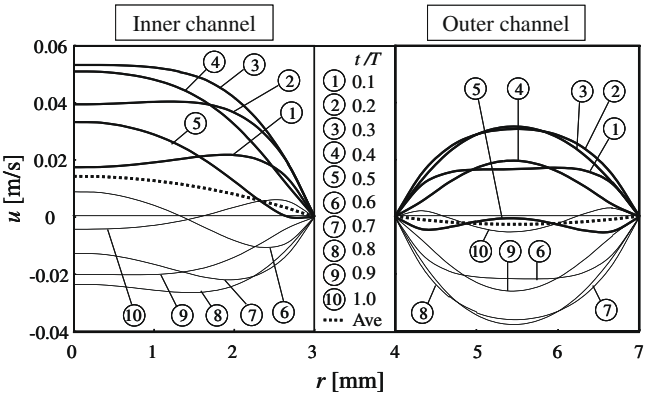

Fig. 7. Variation of u-velocity profiles along middle line of inner and outer channels in one cycle of oscillation (Am = 38.1 mm, f = 0.5 Hz).

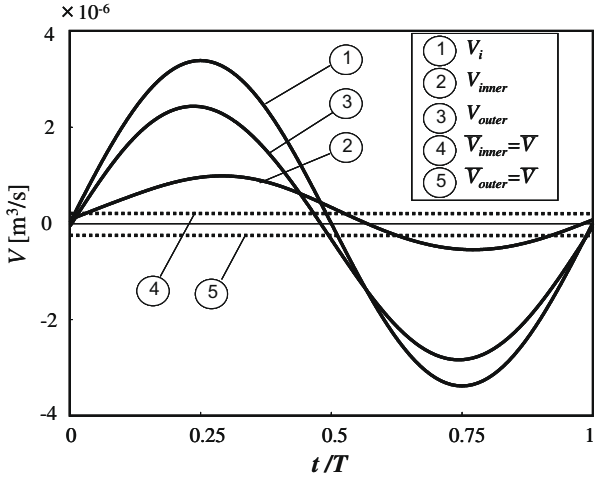

Fig. 8. Variation of flow rate V of oscillatory flow through inner and outer channels in one cycle of oscillation (Am = 38.1 mm, f = 0.5 Hz).

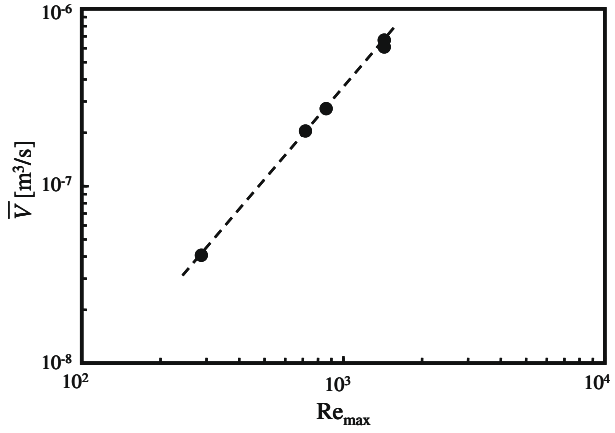

Fig. 9. Relationship between flow rate V of unidirectional flow component through inner and outer channels.

numerical calculation. The total analytical domain was divided into about 13,000–70,000 meshes.

3.2. Analytical results

3.2.1. Flow field

Fig. 6 illustrates the variation of the contour lines of the stream function in one cycle of oscillation in the outer and inner channels. They indicate that the oscillatory flow separated at the left round orifice and generated vortices in the outer channel in the pushing phase ($0 \leqslant t/T \leqslant 0.5$) and the flow separated at the right annular orifice and generated vortices in the inner channel in the pulling phase ($0.5 \leqslant t/T \leqslant 1.0$). It seems that the generation of vortices in the left end of the outer channel caused the higher flow resistance of the outer channel in the pushing phase compared with that in the pulling phase. In a similar way, the separation of the flow at the right end of the channel caused higher flow resistance in the pulling phase than that in the pushing phase in the inner channel. Fig. 6 also indicates that in the middle regions of the inner and outer channels the contour lines were parallel to the wall surfaces and no vortices were observed there.

Fig. 7 illustrates the variation of u-velocity profile along the middle line of the inner and outer channels (refer Fig. 5). The dotted lines are the profile of the time-average u-velocity, that is, the u-velocity averaged in one cycle of oscillation. In the outer channel, the absolute values of the u-velocities in the pulling phase ($0.5 \leqslant t/T \leqslant 1.0$) were larger than those in the pushing phase ($0 \leqslant t/T \leqslant 0.5$), which induced the negative time-averaged u-velocity flowing from the hot water bath to the cold water bath. While, in the inner channel, the positive time-average u-velocity was induced and it was flowing from the cold to the hot water bath. These non-zero time-average u-velocities were caused by the difference of the flow resistances between the pushing and pulling phases in each of the outer and inner channels, as described above. Hereafter, we refer to the non-zero time-average u-velocity as unidirectional flow component. Thus, we can consider that the oscillatory flow induced in the outer and inner channels in the present heat transportation pipe was composed of the unidirectional flow component (non-zero time-average flow component) and the reciprocal flow component. In the inner channel the unidirectional flow component was flowing from the cold to the hot water bath. While, in the outer channel, the unidirectional flow component was flowing from the hot to the cold water bath. As will be described later, the unidirectional flow component induced in the outer channel played an important role in the augmentation of the longitudinal heat transportation in the present double tube type heat transportation pipe.

Fig. 8 shows variation of the flow rates through the inner channel (curve 2) and through the outer channel (curve 3). The flow rates were calculated by integrating u-velocity over one cycle of

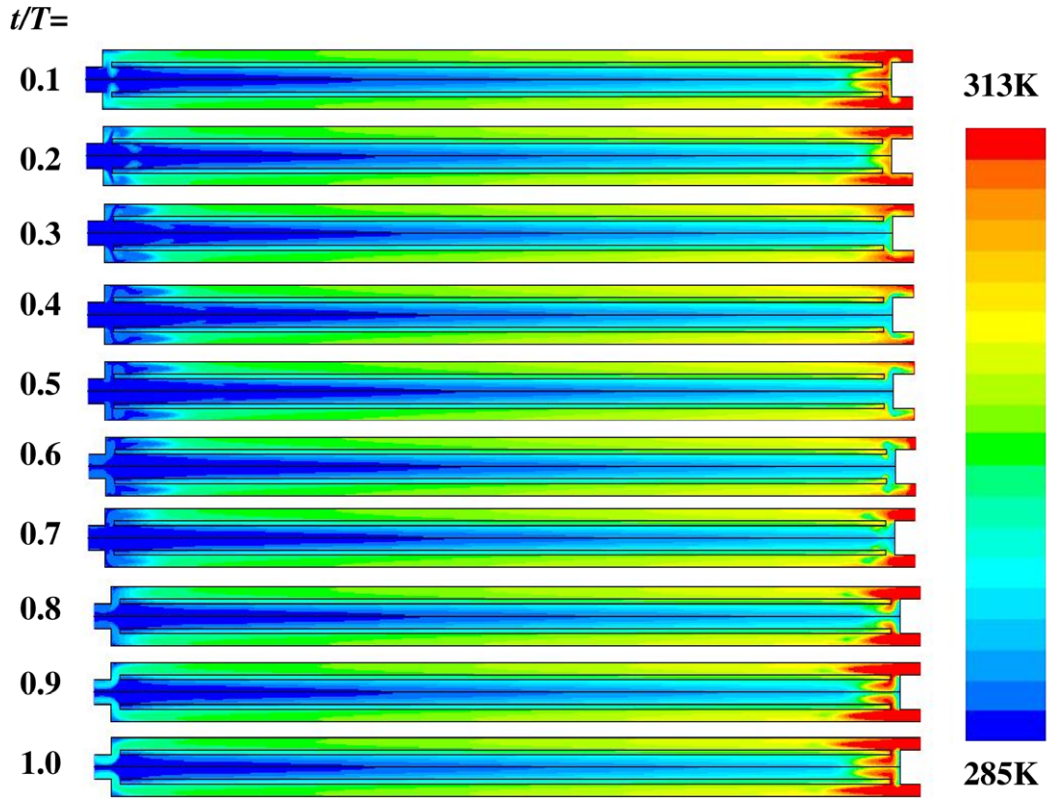

Fig. 10. Variation of temperature field in the heat transportation pipe (Am = 38.1 mm, f = 0.5 Hz).

time and over the entire flow cross-section. The curve 1 shows the flow rate variation of the sinusoidal reciprocal flow imposed on the round orifice at the left end of the tube, which was given by Eq. (15).

$$V_i(t/T) = 2\pi f \cdot Am \cdot \sin(2\pi \cdot t/T) \cdot S_o \quad \text{(refer Eq. (11))} \tag{15}$$

Here, S_o is the cross-sectional area of the left round orifice.

The dotted lines 4 and 5 are the time-average flow rate through the inner and outer channels. The variations of flow rate through the outer and inner channels were expressed by the following equations:

$$V_{outer}(t/T) = \tilde{V}_{outer}(t/T) - \bar{V} \tag{16}$$

$$V_{inner}(t/T) = \tilde{V}_{inner}(t/T) + \bar{V} \tag{17}$$

Here, $\bar{V}$ is the absolute value of the time-average flow rate through the outer and inner channels. Eqs. (16) and (17) mean that the flow rate of the oscillatory flow induced in the outer and inner channels can be expressed as the sum of the flow rates of the reciprocal flow component and the unidirectional flow component. They mean that in the outer channel the unidirectional flow component was flowing toward the cold water bath from the hot water bath, and in the inner channel it was flowing toward the hot water bath from the cold water bath.

In Fig. 9, the absolute vale $\bar{V}$ of the time-average flow rate is plotted against the maximum Reynolds number Re_{max}. $\bar{V}$ increased with increasing Re_{max}.

3.2.2. Temperature field

Figs. 10 and 11 illustrate the variation of the temperature distributions in the inner and outer channels. θ^* in Fig. 11 is the dimensionless temperature defined by Eq. (18). Longitudinal temperature distributions along the center lines of the inner channel at $r = 0$ and the outer channel at $r = 5.5$ are shown in Fig. 11.

$$\theta^* = (\theta - \theta_c)/(\theta_h - \theta_c) \tag{18}$$

The water temperature in the outer channel was higher than that in the inner channel. This was because the unidirectional flow component was flowing from the hot water bath to the cold water bath in the outer channel and it was flowing in the reverse direction in the inner channel.

As shown in Fig. 11, the temperature gradients in the middle part of the outer and inner channels were not zero. The temperature gradients were caused by the overall heat transmission from the outer to the inner channel through heat conduction in the inner acrylic tube. This will be clearly understood by comparing the water temperature fields with and without heat conduction through the inner acrylic tube. The temperature fields without heat conduction in the double tube will be shown in the following chapter.

3.2.3. Heat transportation

The dotted, dashed and solid lines in Figs. 12(a) and (b) show the heat transportation rate $Q_{outer}/\Delta\theta$ through the outer channel, $Q_{inner}/\Delta\theta$ through the inner channel and the total heat transportation rate $Q/\Delta\theta$ ($=Q_{outer}/\Delta\theta + Q_{inner}/\Delta\theta$) in the heat transportation pipe. The positive gradient of $Q_{outer}/\Delta\theta$ and the negative gradient of $Q_{inner}/\Delta\theta$ were caused by the overall heat transmission from the outer to the inner channel through the inner acrylic tube as mentioned before. The positive value of $Q_{outer}/\Delta\theta$ means that the heat was transported from the hot water bath to the cold water bath through the outer channel. The negative value of $Q_{inner}/\Delta\theta$ means that the heat was returned back from the left cold end to the right hot water bath through the inner channel. The negative heat transportation was caused by the unidirectional flow component flowing in the inner channel from the cold to the hot water bath. However, it should be mentioned that Q_{inner} which was returned back to the hot water bath was very small compared to Q_{outer} which was transported from the hot to the cold water bath.

Fig. 13(a) and (b) compares the heat transportation flux through the outer channel by the unidirectional flow component with that by the reciprocal flow component in the outer channel. $\tilde{q}$, $\bar{q}$ and q in Fig. 13 are the heat transportation fluxes by the reciprocal flow component, by the unidirectional flow component and total heat

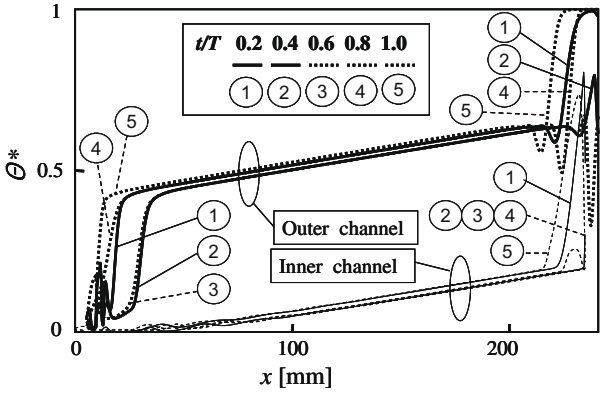

Fig. 11. Variation of temperature field in outer and inner channels (Am = 38.1 mm, f = 0.5 Hz).

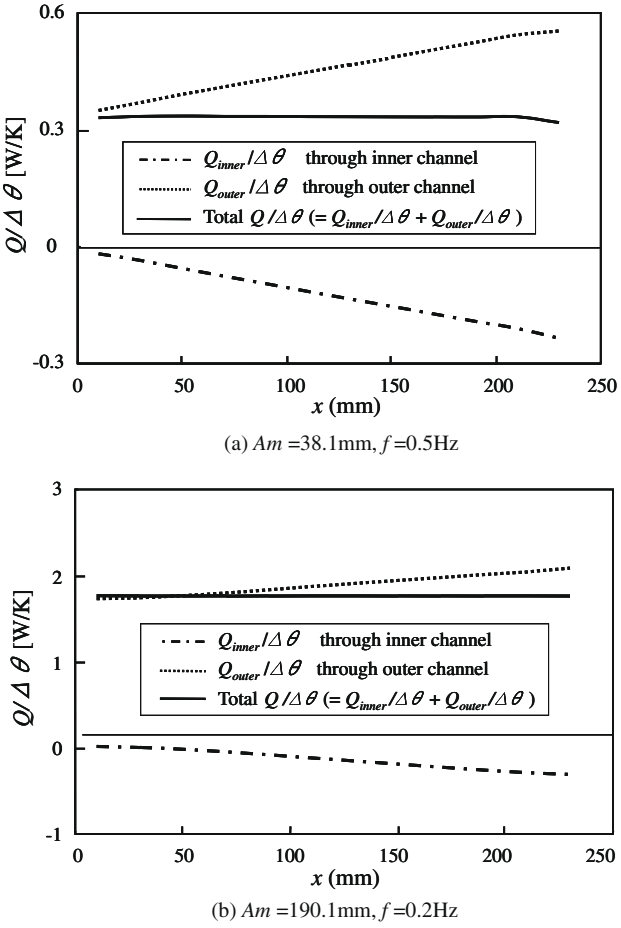

(a) Am =38.1mm, f =0.5Hz

(b) Am =190.1mm, f =0.2Hz

Fig. 12. Heat transportation rates by unidirectional flow component and reciprocal flow component.

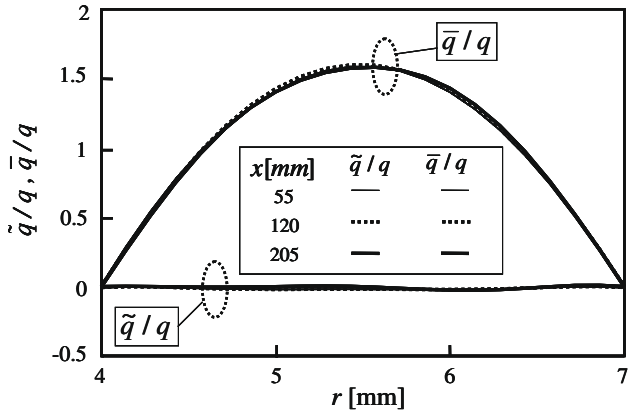

(a) Am =38.1mm, f =0.5Hz

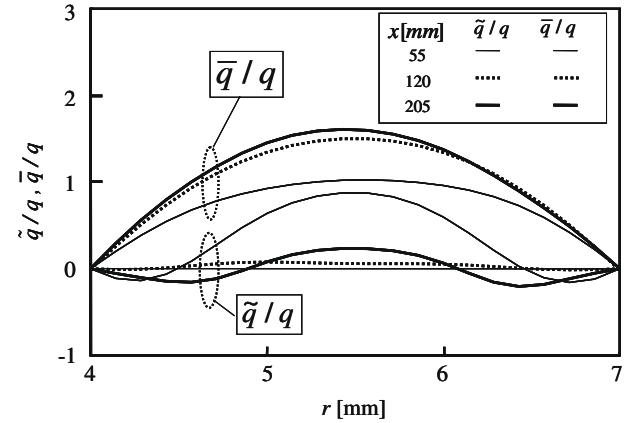

(b) Am =190.1mm, f =0.2Hz

Fig. 13. Heat transportation fluxes by unidirectional flow component and by reciprocal flow component in outer channel.

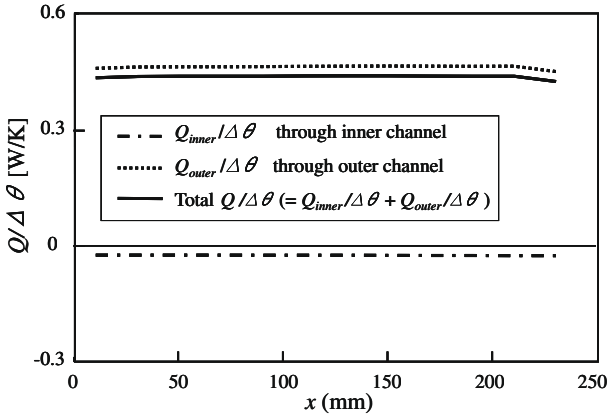

Fig. 14. Heat transportation rates of the heat transportation pipe with adiabatic inner tube (Am = 38.1 mm, f = 0.5 Hz).

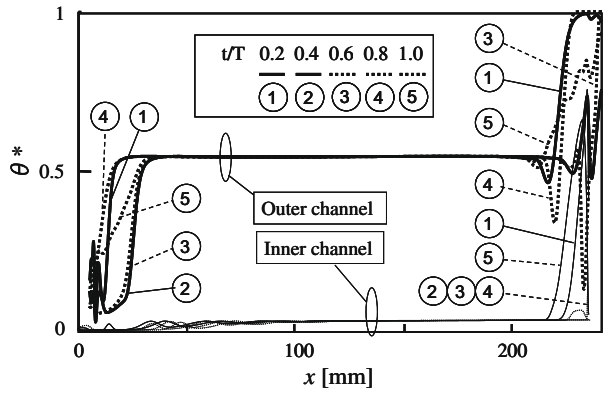

Fig. 15. Variation of temperature field in outer and inner channels for the heat transportation with adiabatic inner tube (Am = 38.1 mm, f = 0.5 Hz).

transportation flux, respectively. $\tilde{q}$, $\bar{q}$ and q were calculated by the following equations:

$$\tilde{q}=\frac{1}{T}\int_t^{t+T}\rho C_p\tilde{u}\,(\theta-\theta_c)\,dt,\quad \bar{q}=\frac{1}{T}\int_t^{t+T}\rho C_p\bar{u}(\theta-\theta_c)dt,\quad q=\tilde{q}+\bar{q} \tag{19}$$

$$u=\tilde{u}+\bar{u} \tag{20}$$

Here, $\tilde{u}$ and $\bar{u}$ are the u-velocity of the reciprocal flow component and that of the unidirectional flow component. Fig. 13 indicates that the heat was mainly transported by the unidirectional flow components in the outer channel, that is, the unidirectional flow component had the significant role in the heat transportation in the outer channel, as well as in the total heat transportation of the double tube (note that the negative heat transportation in the inner channel was very small).

As mentioned before, the black solid circular and triangular symbols in Figs. 2 and 3 are the calculated heat transportation rates. The calculated heat transportation rates agreed well with the experimental ones.

Fig. 14 illustrates the heat transportation rates, $Q_{outer}/\Delta\theta$, $Q_{inner}/\Delta\theta$ and $Q/\Delta\theta$ (=$Q_{outer}/\Delta\theta + Q_{inner}/\Delta\theta$) and Fig. 15 designates the variation of water temperature in the outer and inner channels when the inner tube was completely adiabatic, that is, when there was no overall heat transmissions from the outer to the inner channel. Fig. 15 shows longitudinal temperature distributions along the center lines of the outer channel at r = 5.5 mm and of the inner channel at r = 0 mm. $Q_{outer}/\Delta\theta$ and $Q_{inner}/\Delta\theta$ were uniform along the longitudinal direction of the heat transportation pipe as shown in Fig. 14, and water temperature in the middle part of the outer and inner channels was uniform as shown in Fig. 15. These results were caused by the fact that there was no overall heat transmission from the outer to the inner channel. The calculated result, that water temperature in the middle region of the outer and inner channels had constant value, also means that the unidirectional flow played an important role in the longitudinal heat transportation in the middle region of the present double tube.

In Fig. 16, total heat transportation rate $Q/\Delta\theta$ in the present heat transport pipe are plotted against the flow rate $\bar{V}$ of the

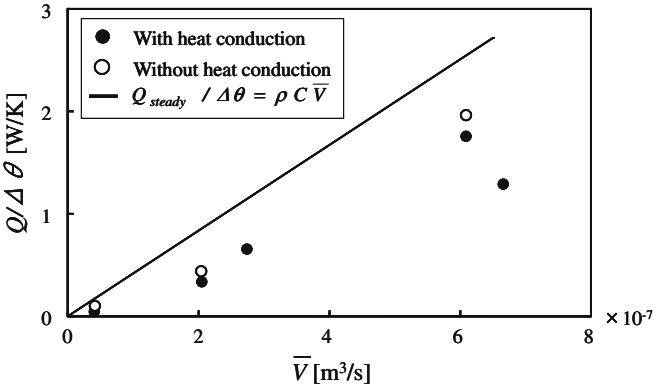

Fig. 16. Relationship between heat transportation rate and flow rate of unidirectional flow component.

unidirectional flow component. Black solid circles are the total heat transportation rate $Q/\Delta\theta$ when there was the overall heat transmission from the outer to the inner channel. Open circles are the heat transportation rate $Q/\Delta\theta$ when there was no overall heat transmission or no heat conduction through the inner acrylic tube. The black straight line designates the heat transportation rate $Q_{steady}/\Delta\theta$ which will be transported by a steady flow whose flow rate was assumed to be $\bar{V}$. The heat transportation rates in the present double tube increased with increasing $\bar{V}$ and they reached about 25–70% of the heat transportation rate Q_{steady} of the assumed steady flow.

4. Conclusion

The present study aims to investigate the heat transportation of a double tube type heat transportation pipe which was proposed by Ishii et al. [9]. Experiments were performed in the ranges of $2.3 \leqslant \mathrm{Wo} \leqslant 7.2$ and $400 \leqslant \mathrm{Re}_{\max} \leqslant 6600$ by varying the frequency f in the range of $0.1 \leqslant f \leqslant 1.0$ Hz and the amplitude of the reciprocal flow Am in the range of $38 \leqslant Am \leqslant 190$ mm. The temperatures of the hot water bath θ_h and the cold water bath θ_c varied from 30 to 40 °C and 8 to 20 °C, respectively, thus the temperature difference $\Delta\theta = \theta_h - \theta_c$ between the hot and cold bathes ranged from 9 to 30 °C. In order to understand the heat transportation mechanism of the present heat transportation pipe, numerical analysis was performed. Main results derived in the present study were summarized in the following:

(1) Heat transportation rate Q of the present double tube type heat transportation pipe increased with an increase in the frequency f and the tidal amplitude Am of the reciprocal flow which was imposed on the left end of the heat transportation pipe. The heat transportation rate Q of the present heat transportation pipe was 10–490 times the heat transportation rate Q_{kav} of the straight round pipe, and Q was approximately 1–40 times the heat conduction rate through the copper rod.

(2) Dimensionless heat transportation rate Q^* was correlated by $Q^* = 0.0252\,\mathrm{Re}_{\max}^{0.3}$.

(3) Analytical results suggest that oscillatory flow induced in the outer and inner channels of the present double tube is composed of the reciprocal flow component and unidirectional flow component. The unidirectional flow component flowing in the outer channel from the hot to the cold water bath significantly augmented the heat transportation rate of the present double tube type heat transportation pipe.

(4) Analytical heat transportation rates agreed well with the experimental ones.

References

[1] U.H. Kurzweg, L. Zhao, Heat transfer by high-frequency oscillations, Phys. Fluids 27 (11) (1984) 2624–2627.
[2] M. Kaviany, Performance of a heat exchanger based on enhanced heat diffusion in fluids by oscillation, Trans. ASME, J. Heat Trans. 112 (1990) 49–55.
[3] S. Nishio, M. Honma, W.M. Zhang, Oscillation-controlled heat transport tube (1st report, Effect of liquid properties), Trans. JSME 60 (569B) (1994) 233–239.
[4] S. Nishio, W.M. Zhang, Oscillation-controlled heat transport tube (2nd report, Optimum condition), Trans. JSME 60 (570B) (1994) 627–633.
[5] S. Nishio, X.H. Shi, K. Funatsu, Study on oscillation-controlled heat transport tube (3nd report, Inverted oscillation-phase heat transport tube), Trans. JSME 60 (578B) (1994) 3498–3503.
[6] Y. Ohno, G. Tanaka, M. Hishida, Enhanced heat transfer during oscillatory flow in annular channel, Trans. JSME 70 (698B) (2004) 2612–2619.
[7] T. Inaba, M. Tahara, K. Saitoh, The effect of the pipe cross-sectional shape on the longitudinal heat transfer in oscillatory flow in pipe bundles, Trans. JSME 65 (636B) (1999) 2821–2827.
[8] Y. Ishii, P. Zhang, R. Kawai, M. Hishida, G. Tanaka, Heat transportation by an oscillatory flow through a new heat transportation pipe, in: Proceedings of the 13th International Heat Transfer Conference, Sydney, Australia, 2006, Paper No. EQP-23.
[9] Y. Ishii, X. Zhang, M. Hishida, Heat transportation by an oscillatory flow through a parallel-plate channel with an inserted slanting plate, in: Proceedings of HT2007, 2007 ASME–JSME Thermal Engineering and Summer Heat Transfer Conference, Canada, 2007, Paper No. HT2007-32561.
[10] T. Motoki, Y. Ohno, M. Hishida, G. Tanaka, Augmentation of thermal energy transportation by an oscillatory flow in grooved ducts, Trans. JSME 72 (721B) (2006) 2271–2278.
[11] FLUENT 6.1, Users Guide, Fluent Inc., 2003.